ELSEVIER

Comparison of different advanced oxidation processes (AOPs) in the presence of perovskites

F.J. Rivas [a,*], M. Carbajo [a], F. Beltrán [a], O. Gimeno [a], J. Frades [b]

[a] *Departamento de Ingeniería Química y Química Física, Universidad de Extremadura, Avenida de Elvas S/N, 06071 Badajoz, Spain*
[b] *Departamento de Ingeniería Química, Universidad de Castilla la Mancha, Plaza de Manuel Meca s/n 13400 Almadén, Ciudad Real, Spain*

Abstract

The efficacy of the oxidation systems: O_3, UV radiation, O_3/UV radiation, O_3/perovskite, UV radiation/perovskite, O_3/UV radiation/perovskite, H_2O_2/UV radiation, H_2O_2/UV radiation/perovskite, has been investigated by using pyruvic acid as probe compound. Under the operating conditions used, the combination of UV radiation and hydrogen peroxide (with or without perovskites) leads to the fastest pyruvic acid removal while the best results in terms of mineralization degree are obtained when combining O_3/UV radiation/perovskite. The effect of the variables: inlet ozone (15–$75\,mg\,L^{-1}$) and initial pyruvic acid (10^{-3} to $10^{-2}\,M$) concentrations, catalyst load (0.01–$1.5\,g\,L^{-1}$) and pH (2–9) was investigated for the photocatalytic ozonation. The most influencing parameter was the ozone concentration fed to the photoreactor. A zero order was observed for pyruvic acid concentration and close to zero for catalyst load. Some deactivation is observed after reusing the catalyst, likely due to leaching of the active phase.
© 2007 Elsevier B.V. All rights reserved.

Keywords: Perovskite; Ozone; Pyruvic acid; AOPs; UV radiation

1. Introduction

Advanced oxidation processes (AOPs) have typically been defined as those water cleaning technologies that involve the formation of powerful oxidizing agents (commonly hydroxyl radicals) capable of unselectively reacting with the organic (and in some cases inorganic) content of the aqueous effluents [1]. AOPs are usually applied to eliminate micropollutants present in relatively "clean" waters, although under some circumstances they have also been used to improve the biodegradability properties of wastewaters.

Application of AOPs is governed by several factors (organic load, water transparency to radiation, radical inhibitor presence, etc.). AOPs are established as "destructive" water treatment technologies. Thus, contrarily to other tertiary processes (i.e. adsorption processes, membrane processes, etc.) they transform harmful substances into water and carbon dioxide, or, alternatively into other harmless byproducts. They constitute an

alternative to biological processes when biotoxic substances are present in the effluents. Additionally, AOPs are capable of mineralizing a wide range of micropollutants, avoiding the accumulation of oxidation end products [2].

If the latter task (high degree of mineralization) is to be fulfilled, it is a common practice to combine several oxidation systems. The integration of photolysis and ozonation processes in a single stage leads to the appearance of an effective treatment (photolytic ozonation) involving the simultaneous development of two direct routes of pollutant elimination (direct photolysis and direct ozonation) plus three routes of radical formation (ozone decomposition with hydroxyl and perhydroxyl anions and hydrogen peroxide photodecomposition). The system O_3/UV radiation offers the advantages of the pairs O_3/OH^-, O_3/H_2O_2 and H_2O_2/UV radiation [3].

As a rule of thumb, at the expense of a higher cost, the more complex a system is (i.e. higher number of single oxidation types), the higher its efficiency. However, AOPs can increase their efficacy, with almost no additional cost in operating expenses, if a suitable heterogeneous catalyst is used. When the system O_3/UV radiation is used, addition of a heterogeneous solid to the reaction media should either

* Corresponding author. Tel.: +34 924289385; fax: +34 924289385.
E-mail address: fjrivas@unex.es (F.J. Rivas).

catalyze ozone decomposition and/or be an effective photocatalyst.

Perovskites of the type $LaTi_{0.15}Cu_{0.85}O_3$ have successfully been used in catalytic ozonation processes of ozone refractory compounds. In the present paper this kind of catalyst has been used in combination with several oxidation systems so any synergistic effect could be envisaged. Because of its higher efficacy, the system O_3/UV radiation in the presence of perovskites has been investigated in more detail. For so doing, pyruvic acid was adopted as a model compound of recalcitrant compounds towards ozonation processes [4].

2. Experimental

All the experiments were carried out in semibatch mode. The photoreactor was a cylindrical glass vessel equipped with a porous plate to bubble oxygen or an oxygen–ozone mixture, sampling port with a syringe, thermometer, outlet gas and magnetic agitation. Temperature was kept controlled at $20 \pm 0.1\,°C$ by immersion of the reactor into a thermostatic batch. Ozone was produced from an *Erwin Sander 301.7* laboratory ozone generator. UV radiation was generated by a low-pressure mercury lamp Heraeus Hanau TNN 15/32 located in the middle of the reactor. When needed, the finely divided solid catalyst (perovskites) was used in slurry mode.

Throughout an experiment, samples were withdrawn from the reactor and analyzed for the parent compound (pyruvic acid), intermediate content (acetic and oxalic acids), total organic carbon (TOC) evolution and dissolved ozone concentration.

Dissolved ozone was measured before solid filtration by following the method proposed by Bader and Hoigne [5] based on the decoloration of the 5,5,7-indigotrisulphonate. For that purpose a Thermo Spectronic Heλios α spectrophotometer was used. Additionally, ozone in the gas phase was monitored by means of an Anseros Ozomat ozone analyzer. Total carbon (TC) and TOC were monitored by an IR carbon analyzer after persulphate oxidation of the aqueous samples (I/O Analytic 1010 apparatus).

Pyruvic acid and oxidation byproducts (Sigma–Aldrich) were determined by HPLC (Hewlett Packard Series 1100). The mobile phase pumped through a Supelcogel 610-H column was pure water at pH 2.5 (1% in phosphoric acid). Detection of organics was carried out at 210 nm. Reaction media pH was measured by utilizing a Crison 507 pH-meter.

The catalyst was prepared as follows. $LaTi_{0.15}Cu_{0.85}O_3$ was obtained by citrate decomposition from a concentrated solution of $La(NO_3)_3 \cdot 6H_2O$ $(20.6 \times 10^{-3}\,M)$ mixed with $Cu(NO_3)_2 \cdot 3H_2O$ with a ratio Cu:La = 0.85. After mixing at $0\,°C$, a titanium but oxide solution in isopropyl alcohol was slowly added to get a Ti:La ratio = 0.15. Thereafter, citric acid was added to introduce the stoichiometric amount of citrates in the media to form the corresponding metal complexes. The final pH after the whole process was around 2–3. The previous dispersion after agitation was dried under mild conditions of temperature. The gel obtained was finally kept at $110\,°C$ for 24 h and calcined at $700\,°C$. Additional details of the solid surface nature and preparation can be found elsewhere [6].

3. Results and discussion

3.1. Comparison of AOPs

The efficiency of the oxidation systems: O_3, UV radiation, O_3/UV radiation, O_3/perovskite, UV radiation/perovskite, O_3/UV radiation/perovskite, H_2O_2/UV radiation, H_2O_2/UV radiation/perovskite, has been investigated by following the evolution profiles of pyruvic acid and TOC with the reaction time. Fig. 1 shows the results obtained in the aforementioned experimental series.

As expected [6,7], ozone is not capable of appreciably remove pyruvic acid from the media after 3 h of reaction, showing conversion values slightly above 20%. Nevertheless, application of
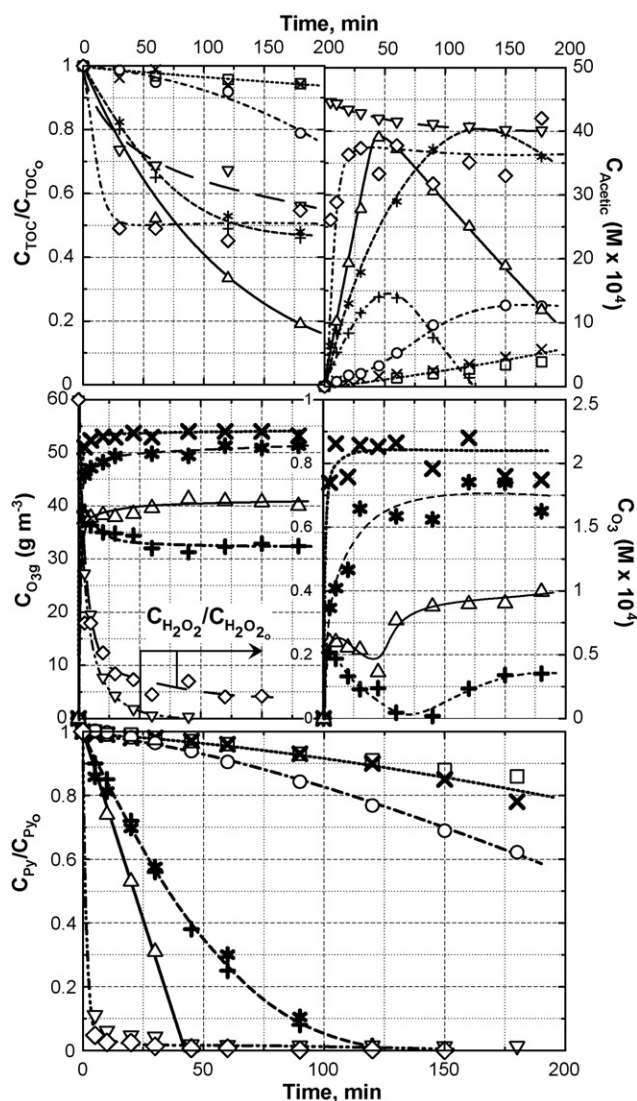

Fig. 1. Oxidation of pyruvic acid. Comparison of different oxidation systems. Experimental conditions: pH 7, $Q_{O_2-O_3} = 40\,L\,h^{-1}$, $C_{O_3g(inlet)} = 50\,g\,m^{-3}$, $C_{Perovskite} = 1\,g\,L^{-1}$, $C_{py_o} = 5 \times 10^{-3}\,mol\,L^{-1}$, $T = 293\,K$, $I_o = 4.5 \times 10^{-6}\,Einstein\,L^{-1}\,s^{-1}$ and $L = 4.5\,cm$. Symbols: (×) O_3; (○) UV radiation; (∗) O_3/perovskite; (□) UV radiation/perovskite; (+) O_3/UV radiation; (△) O_3/UV radiation/perovskite; (▽) UV radiation/H_2O_2; (◇) UV radiation/H_2O_2/perovskite.

UV radiation with an intensity of 4.56×10^{-6} Einstein $L^{-1}\,s^{-1}$ and a radiation path of $4.5\,cm$ leads to a roughly 40% of pyruvic acid elimination. The latter results are somehow unexpected given the low extinction coefficient of the organic acid ($87\,M^{-1}\,cm^{-1}$, $R^2 = 0.999$), indicating, therefore, that the quantum yield must be relatively high. Addition of perovskites to the aqueous solution involves the partial inhibition of the photolytic process. Therefore, the solid, rather than acting as a photocatalyst, provokes a shielding effect in the applied radiation. The behaviour is the opposite if perovskites are added when pyruvic acid is ozonated. As already reported [6], this catalyst is capable of accelerating the acid abatement by surface catalyzing the ozone decomposition into more reactive species. A similar effect was also experienced when photolysing ozone. In the latter situation pyruvic acid is decomposed by direct ozonation, direct photolysis, and indirectly by hydroxyl radicals formed in the photolysis of the hydrogen peroxide generated after ozone radiation. The systems O_3/UV radiation and O_3/perovskite lead to analogous results both in terms of pyruvic acid elimination and TOC decrease. However, given the proven stability of the solid catalyst in ozonation processes [8], the catalytic ozonation is preferred to the photolytic ozonation. The choice is mainly based on economic reasons. Thus, not only the catalyst is cheaper than UV radiation but also the ozone uptake is lower in the O_3/perovskite process if compared to the O_3/UV radiation oxidation (see Fig. 1).

The integration of catalytic ozonation and UV radiation offers the advantages of the systems UV radiation, O_3/UV radiation and O_3/perovskite. In the combination of the oxidants O_3/UV radiation/perovskite, pyruvic acid is completely eliminated in just 45 min while the TOC abatement is increased to roughly 80% in 180 min of reaction. The trend observed in Fig. 1 indicates that total mineralization of the sample can be achieved if the reaction time is extended above 3 h.

The promising performance of the O_3/UV oxidation system suggests that the UV/H_2O_2 combination should also work with pyruvic acid. In fact, given that the direct ozonation of the organic acid is negligible, the pairs O_3/UV and UV/H_2O_2 reduce to the same, i.e. direct photolysis of pyruvic acid plus hydroxyl radical attack formed from the homolytic scission of the H_2O_2 molecule in the presence of ultraviolet radiation. The previous hypothesis was confirmed in Fig. 1. Thus, the initial presence of 5×10^{-3} M of hydrogen peroxide involves the 90–95% of pyruvic acid oxidation in less than 5 min form the start of the process. Given the fast removal of pyruvic acid, addition of perovskites to the UV/H_2O_2 process involves a negligible effect in its abatement rate. Some differences are found, however, in the case of the mineralization degree obtained. Hence, when perovskites are present, the TOC conversion rate observed in the first 30 min is the highest amongst all the oxidant combinations tested. However, TOC decrease comes to a halt when H_2O_2 is consumed (see Fig. 1). The final TOC removal achieved with the system UV/H_2O_2/perovskite is analogous to the UV/H_2O_2 combination.

The only two intermediates detected when oxidizing pyruvic acid are oxalic and acetic acids. Nonetheless, with the exception of the system O_3/UV, the selectivity towards acetic acid

is close to 100%. Fig. 1 shows the evolution profiles of the acetic acid formed from pyruvic acid oxidation. From this figure some aspects should be highlighted. Thus, acetic acid immediately accumulates in the UV/H_2O_2/perovskite and UV/H_2O_2 systems with values approaching 70–80% of the initial pyruvic acid present in solution. Neglecting the contribution of oxalic acid, theoretically, the normalized TOC concentration should be $(0.7–0.8) \times 2/3 = (0.47–0.53)$ which agrees well with the experimentally measured TOC. In spite of the coincidence in performance of the pairs O_3/UV and O_3/perovskite, the acetic acid profiles clearly indicate a different mechanism taking place. Hence, as stated previously, the selectivity of the oxidation towards acetic acid significantly decreases in the photolytic ozonation. The concentration of this acid shows a maximum at 50 min ($\approx 1.5 \times 10^{-3}$ M) decreasing, thereafter to the complete disappearance in roughly 125 min of treatment. When the catalytic ozonation is applied, the maximum obtained is higher ($\approx 4.0 \times 10^{-3}$ M) and delayed to 125 min. The photocatalytic ozonation of pyruvic acid leads to the fast formation of acetic acid with a maximum of around 4.0×10^{-3} M at 50 min and, also, a relatively fast decrease of this acid at a constant rate of 2×10^{-5} M min^{-1}.

Once analyzed the efficacy of the different oxidation processes studied, under the operating conditions investigated, it can be concluded that the photocatalytic ozonation of pyruvic acid is, *a priori*, the best option. A simplistic economic analysis of the operating costs associated to each system would corroborate the previous statement [9]. The economic study presented is just an approximate tool to differentiate between the operating costs associated to the use of each oxidation system. Obviously, figures presented in this simplified scheme should be considered in relative terms rather than absolute values. Thus, those systems using oxygen should consider that the oxygen cylinders have a cost of €$5.55\,m^{-3}$ O_2 (including taxes), having to add transport (€17.5 for a $10.6\,m^3$ cylinder) and cylinder rental (€$0.545\,day^{-1}$). Adding up all the terms: oxygen cost $= (€5.55\,m^{-3} \times 40 \times 10^{-3}\,m^3\,h^{-1} + 17.5/€10.6\,m^{-3} \times 40 \times 10^{-3}\,m^3\,h^{-1} + €0.545\,day^{-1} \times 1/24\,day\,h^{-1}) \times t$ (h). Electricity cost associated to ozone production is calculated as follows. The maximum ozone production of the ozone generator used is $12\,g\,h^{-1}$. The ozone mass flow rate utilized in this work is $2\,g\,h^{-1}$, that is, a 16.67% of the maximum mass flow rate. According to manufacturers the current consumption is: $16.67/186 = 90\,mA$. As a consequence the ozone production cost $= [220\,V \times 90 \times 10^{-3}\,A \times t$ (h)] kWh $\times$ €$0.0753\,kWh^{-1}$. UV radiation from the low pressure mercury lamp has a cost $= 15 \times 10^{-3}\,kW \times t$ (h) $\times$ €$0.0753\,kWh^{-1}$. Finally, H_2O_2 30% (w/w) has been given an average price of €$17.5\,L^{-1}$. As stated previously, this analysis is just an oversimplified tool to assess the trends in the expenses at the time of implementing the different AOP processes. A rigorous economic analysis should consider the initial investment, prices at plant scale, etc. Fig. 2 displays the trends followed by costs as a function of the removal percentage of pyruvic acid and TOC. In the first case, it is observed how the combination of UV radiation and hydrogen peroxide (in the presence or absence of
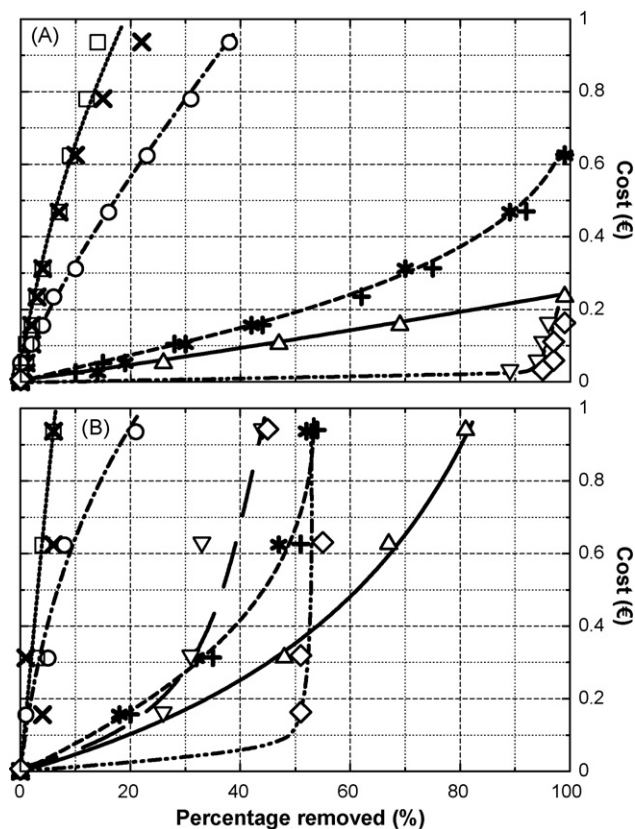
Fig. 2. Oxidation of pyruvic acid. Comparison of different oxidation systems. (A) Costs associated to pyruvic acid removal. (B) Costs associated to TOC removal. Experimental conditions and symbols as in Fig. 1.

perovskites) is the cheapest option regardless of the pyruvic acid conversion achieved. Only for conversions close to 100% the system O_3/UV/perovskite approaches the economic figures of the hydrogen peroxide photolysis. Nevertheless, if TOC abatement is considered, mineralization degrees above 50% indicate that the photocatalytic ozonation is the only suitable technology (under the operating conditions used in the present work).

Consequently, it was decided to carry on this investigation by analyzing the effect of some important operating variables in the process O_3/UV radiation/perovskite.

3.2. The system: O_3/UV radiation/perovskite

3.2.1. Influence of catalyst load

The effect of perovskite loading was investigated in the interval 0.01–1.5 g L^{-1}. Fig. 3 illustrates the results obtained. As observed, catalyst loading seems to exert a negligible influence in the pyruvic acid conversion. Data points for this experimental series lie within a ±20% of the average conversion at each time. Perhaps, a slight poorer efficiency can be envisaged for the run conducted with the lowest catalyst concentration, however, there is no clear trend for the rest of experiments, and it can be concluded that results obtained with different perovskite concentrations are statistically similar. An analogous analysis can be applied to the evolution of TOC, although in this case the experiment with the highest perovskite concentration leads to slightly poorer results than the rest of experiments. The trend observed follows certain linearity with final conversions (after 180 min) of 94, 89, 84, 81 and 79% for increasing values of catalyst concentration. The reason seems to be the opposite effect at increasing concentrations of perovskites. Thus, on one hand,
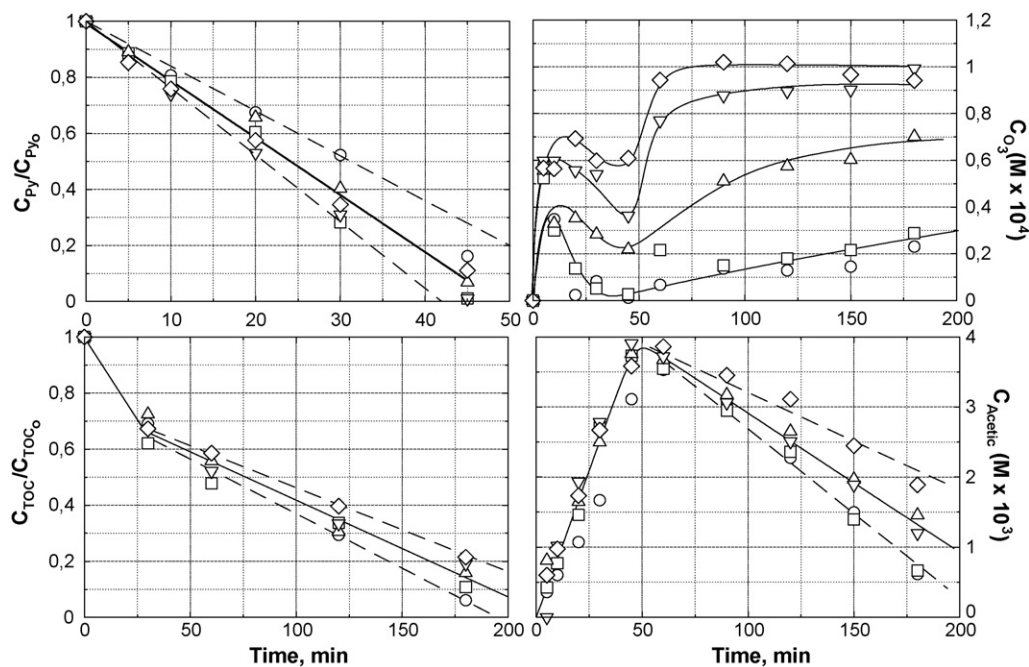

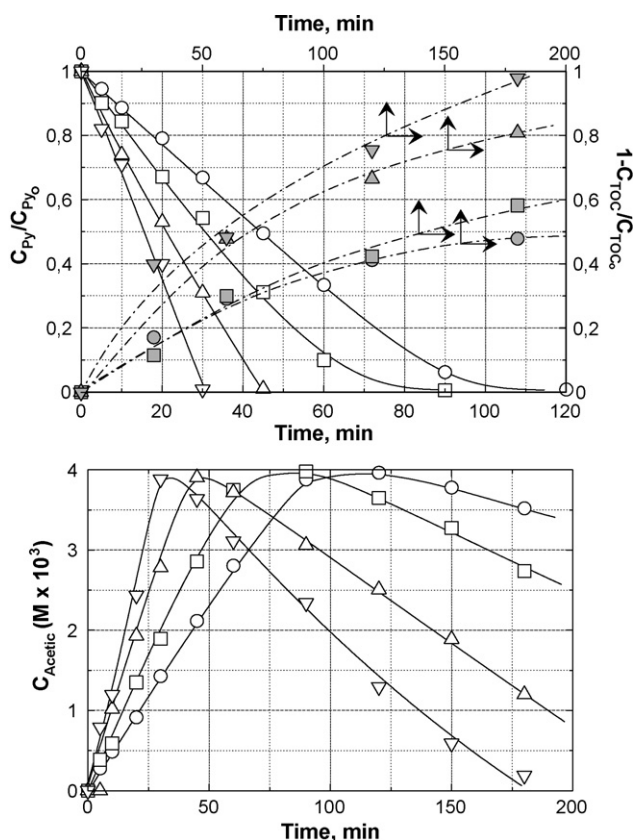Fig. 3. Oxidation of pyruvic acid. Effect of catalyst load in the system O_3/UV radiation/perovskite. Experimental conditions: pH 7, $Q_{O_2-O_3} = 40$ L h^{-1}, $C_{O_3 g(inlet)} = 50$ g m^{-3}, $C_{py_o} = 5 \times 10^{-3}$ mol L^{-1}, $T = 293$ K, $I_o = 4.5 \times 10^{-6}$ Einstein L^{-1} s^{-1} and $L = 4.5$ cm. Symbols: $C_{Perovskite}$ (g L^{-1}), ($\bigcirc$) 0.01; ($\square$) 0.0625; ($\triangle$) 0.2; ($\triangledown$) 1.0; ($\lozenge$) 1.5.

6.2×10^{-5}, 8.7×10^{-5} and 12.6×10^{-5} M min^{-1} for increasing values of inlet ozone concentration. Analogously the acetic acid decomposition rates were 0.67×10^{-5}, 1.4×10^{-5}, 2.0×10^{-5} and 2.6×10^{-5} M min^{-1} also for increasing values of $C_{O_3 g(inlet)}$.

3.2.3. Influence of initial pyruvic acid concentration

Fig. 5 shows the dimensionless pyruvic acid concentration for experiments completed in the presence of different initial amounts of the acid. At a given time, the conversion achieved is higher as the initial concentration of pyruvic acid is decreased. Nevertheless, the true kinetics of the process reveals a zero order regarding the organic acid with constant values of pyruvic acid disappearance of the order of 10^{-4} M min^{-1} independently of its initial concentration. These results are similar to those reported for the catalytic ozonation of pyruvic acid in the presence of perovskites [6]. Moreover, as seen in Fig. 5, acetic acid concentration shows similar rate values of formation (8.4×10^{-5} M min^{-1} close to pyruvic acid removal rate) and decomposition (2×10^{-5} M min^{-1}) for experiments carried out with different initial acid concentration.

3.2.4. Influence of pH

The initial pH effect was investigated in the range 2–9. Fig. 6 depicts the evolution profiles of normalized pyruvic acid concentration, TOC conversion and acetic acid
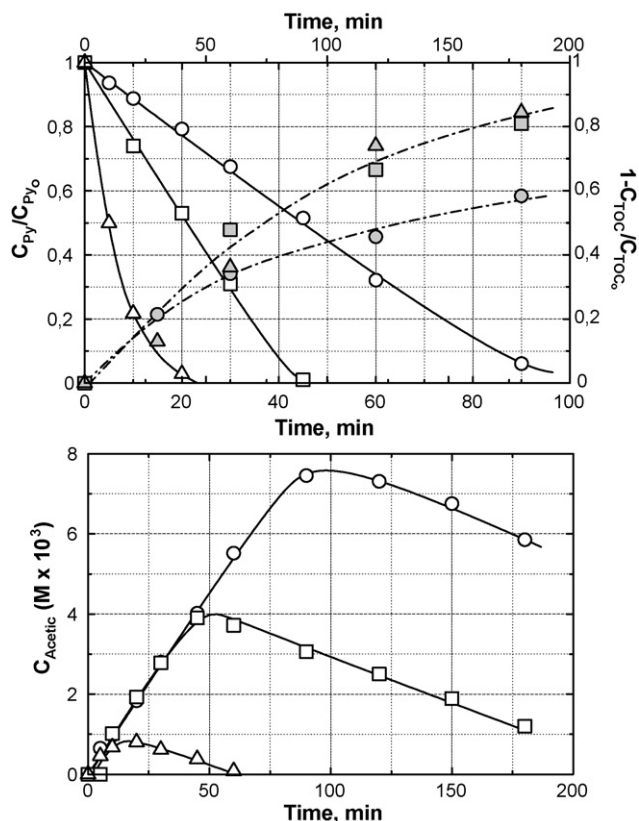
Fig. 4. Oxidation of pyruvic acid. Effect of inlet ozone concentration in the system O$_3$/UV radiation/perovskite. Experimental conditions: pH 7, $Q_{O_2-O_3} = 40$ L h^{-1}, $C_{Perovskite} = 1.0$ g L^{-1}, $C_{py_o} = 5 \times 10^{-3}$ mol L^{-1}, $T = 293$ K, $I_o = 4.5 \times 10^{-6}$ Einstein L^{-1} s^{-1} and $L = 4.5$ cm. Symbols: $C_{O_3 g(inlet)}$ (g m^{-3}), (○) 15; (□) 30; (△) 50; (▽) 75 (solid symbols: TOC conversion).

a higher amount of catalyst enhances the catalytic ozonation, however, on the other hand, the shielding effect towards UV radiation is more pronounced. These small differences are magnified when examining dissolved ozone concentration. Amazingly, the amount of accumulated ozone in the aqueous phase increases as the solid concentration is augmented.

3.2.2. Influence of inlet ozone concentration

The effect of inlet ozone concentration was studied by changing this parameter in the interval 15–75 mg L^{-1}. Fig. 4 illustrates the results obtained. As observed, ozone concentration does exert a positive influence in the pyruvic acid removal rate as well as in the TOC decrease. Thus, after 30 min of reaction conversion values for pyruvic acid are roughly 100, 70, 45 and 35% for experiments conducted by injecting 15, 30, 50 and 75 mg L^{-1} of ozone, respectively. The corresponding TOC conversions for the same runs after 180 min were 98, 80, 60 and 50%. The higher efficiency obtained for increasing values of the inlet ozone concentration is also corroborated by the acetic acid profiles. In all cases, acetic acid curves show a maximum whose value is independent of ozone concentration (around 4×10^{-3} M). However, the time at which the maximum is achieved (i.e. the acetic acid formation rate) and the acetic acid abatement rate increases as the inlet ozone concentration is raised. The rate at which acetic acid was formed was calculated as 4.4×10^{-5},

Fig. 5. Oxidation of pyruvic acid. Effect of initial pyruvic concentration in the system O$_3$/UV radiation/perovskite. Experimental conditions: pH 7, $Q_{O_2-O_3} = 40$ L h^{-1}, $C_{Perovskite} = 1.0$ g L^{-1}, $C_{O_3 g(inlet)} = 50$ g m^{-3}, $T = 293$ K, $I_o = 4.5 \times 10^{-6}$ Einstein L^{-1} s^{-1} and $L = 4.5$ cm. Symbols: C_{py_o} (mol L^{-1}), (○) 0.01; (□) 0.005; (△) 0.001 (solid symbols: TOC conversion).
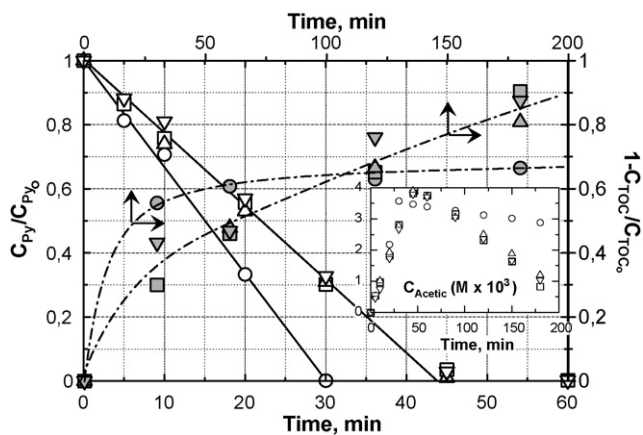
Fig. 6. Oxidation of pyruvic acid. Effect of pH in the system O_3/UV radiation/perovskite. Experimental conditions: $Q_{O_2-O_3} = 40\,L\,h^{-1}$, $C_{O_3g(inlet)} = 50\,g\,m^{-3}$, $C_{Perovskite} = 1.0\,g\,L^{-1}$, $C_{py_o} = 5 \times 10^{-3}\,mol\,L^{-1}$, $T = 293\,K$, $I_o = 4.5 \times 10^{-6}\,Einstein\,L^{-1}\,s^{-1}$ and $L = 4.5\,cm$. Symbols: pH ($\bigcirc$) 2.0; ($\square$) 5.0; ($\triangle$) 7.0; ($\triangledown$) 9.0 (solid symbols: TOC conversion).

formation–decomposition. Excluding pH 2, the rest of pH values seem to exert a negligible influence on the oxidation process (notice that the rest of pHs are above the pK_a value for pyruvic acid). At pH 2, pyruvic acid is more rapidly removed than in the rest of cases (likely due to a better adsorption), however, the TOC conversion comes to a halt after 20–25 min of reaction. Acetic acid decomposition confirms the previous results (see inset figure). The reason for the poorer performance of the catalyst after 20–25 min seems to be the deactivation of the catalyst due to copper leaching.

3.2.5. Catalyst stability

Catalyst stability was assessed by carrying out three consecutive experiments with the same solid after drying it. Fig. 7 illustrates how the activity of the catalyst does not deteriorate after three reuses in terms of pyruvic acid conversion, however, some decrease in TOC conversion is envisaged due to the poorer activity to mineralize acetic acid. Catalyst deactivation is likely related to leaching of the active phase of the solid. More work
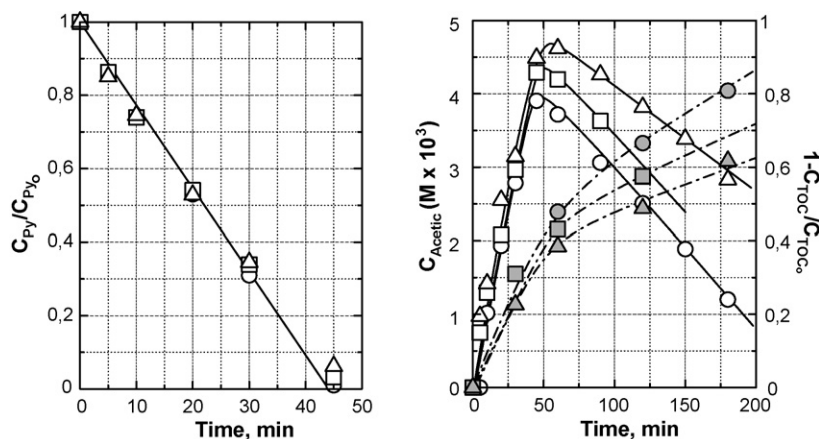
should be done, however, to assess the degree of deactivation achieved after more reuses and the potential relationship to pH.

3.3. Kinetic considerations

The system O_3/UV radiation/perovskite can be initially considered as the addition of the following contributions: photolysis + ozonation + catalytic ozonation + photolytic ozonation. Accordingly, it was decided to account for each individual process and thereafter to check for the result of the addition.

Photolysis of pyruvic acid was modelled by the following expression directly derived from the Lambert–Beer law [9]:

$$-\frac{dC_i}{dt} = \phi_i F_i I_o [1 - \exp(-2.303 L \sum_j \varepsilon_j C_j)] \qquad (1)$$

defining

$$F_i = \frac{\varepsilon_i C_i}{\sum_j \varepsilon_j C_j} \qquad (2)$$

where ϕ_i, ε_i, I_o and L stand for the quantum yield and molar extinction coefficient of compound "i", the incident photon flux by reactor volume unit and the effective optical path in the reactor, respectively. If acetic acid (main intermediate) UV absorption is neglected, $F_i = 1$. Expression (1) was therefore numerically integrated and ϕ_i adjusted to fit experimental and calculated data. The value of ϕ_i found was 2.3 mol Einstein^{-1}.

The ozonation of pyruvic acid is hypothesized to develop in the slow regime. The previous statement is based on the instantaneous appearance of dissolved ozone and the sluggish removal of the acid. Accordingly, the simple second order Eq. (3) applies (the indirect route of hydroxyl radicals attack is neglected):

$$-\frac{dC_{Py}}{dt} = k_{O_3} C_{Py} C_{O_3} \qquad (3)$$

Since C_{O_3} immediately reaches a plateau, Eq. (3) can be transformed into a pseudo first order kinetics of the type:

$$-\frac{dC_{Py}}{dt} = k'_{O_3} C_{Py} \qquad (4)$$

Fig. 7. Oxidation of pyruvic acid. Effect of catalyst reuse in the system O_3/UV radiation/perovskite. Experimental conditions: pH 7, $Q_{O_2-O_3} = 40\,L\,h^{-1}$, $C_{O_3g(inlet)} = 50\,g\,m^{-3}$, $C_{Perovskite} = 1.0\,g\,L^{-1}$, $C_{py_o} = 5 \times 10^{-3}\,mol\,L^{-1}$, $T = 293\,K$, $I_o = 4.5 \times 10^{-6}\,Einstein\,L^{-1}\,s^{-1}$ and $L = 4.5\,cm$. Symbols: number of reuses ($\bigcirc$) 0; ($\square$) 1; ($\triangle$) 2 (solid symbols: TOC conversion).

moreover, since dissolved ozone concentration is close to the ozone concentration in the gas liquid inter-phase ($C_{O_3}^*$), the following approximation can be used, so the potential errors associated to C_{O_3} analysis are reduced:

$$k_{O_3} C_{O_3} \approx k_{O_3} C_{O_3}^* \approx k_{O_3}' \qquad (5)$$

$C_{O_3}^*$ was calculated form the ozone gas outlet concentration and Henry's constant. Taking into account the previous steps, k_{O_3} was calculated to minimize the differences between experimental and calculated pyruvic acid profiles. The value for the direct ozonation was in the proximity of $5\,\mathrm{M}^{-1}\,\mathrm{min}^{-1}$. Notice that if zero order kinetics regarding pyruvic acid had been considered, a value of $0.023\,\mathrm{min}^{-1}$ would have been obtained, similar to the reported value of $0.025\,\mathrm{min}^{-1}$ given by Beltran et al. [7].

The kinetics of the catalytic ozonation of pyruvic acid in the presence of perovskites has already been reported [6]. The following expression was suggested:

$$-\frac{dC_{Py}}{dt} = \frac{k_A C_{O_3}^*}{1 + k_B C_{O_3}^*} \qquad (6)$$

Rivas et al. [6] proposed a value of $k_A = 0.0837\, C_{Cat}(\mathrm{g\,L^{-1}}) + 0.0956\, M_{Py}\, M_{O_3}^{-1}\,\mathrm{min}^{-1}$ and $k_B = 4000 \pm 500\, M_{O_3}^{-1}$. In this work, after fitting the rate constants involved in Eq. (6) the values of 0.5 and 4×10^3 were obtained for k_A and k_B, respectively. Differences between reported values for k_A and the one calculated in this work seem to be the consequence of the difficulties in obtaining exactly the same perovskite in each preparation at laboratory scale (i.e. some of them are more active than others).

Finally, the photolytic ozonation of organics includes a complex reaction mechanism involving several elemental stages. Key steps in this mechanism are basically the formation of hydrogen peroxide through photolysis of molecular ozone and further scission of H_2O_2 to generate two hydroxyl radicals after irradiation [3]. Other routes of HO$^\bullet$ formation are ozone decomposition by hydroxyl anion and ozone decomposition by the ionic form of H_2O_2, which, under the pH operating condition used in this work, can be considered negligible. Consequently, a rough analysis of the system O_3/UV radiation might hypothesize

that HO$^\bullet$ radical concentration in this system can be considered to be proportional to H_2O_2 in the liquid phase and inversely proportional to the routes of HO$^\bullet$ consumption:

$$C_{HO^\bullet} = \alpha \frac{C_{H_2O_2}}{k_{HO^\bullet,Py} C_{Py} + k_{HO^\bullet,Ac} C_{Ac} + k_{HO^\bullet,O_3} C_{O_3} + k_{HO^\bullet,H_2O_2} C_{H_2O_2}} \qquad (7)$$

Additionally, hydrogen peroxide formation is the result of ozone photolysis:

$$O_3 + H_2O \xrightarrow{h\nu} H_2O_2 + O_2 \qquad (8)$$

Accordingly, the following proportionalities can be suggested:

$$C_{H_2O_2} \propto C_{O_3} \propto C_{O_3}^* \qquad (9)$$

Therefore:

$$C_{HO^\bullet} = \beta \frac{C_{O_3}^*}{k_{HO^\bullet,Py} C_{Py} + k_{HO^\bullet,Ac} C_{Ac} + k_{HO^\bullet,O_3} C_{O_3} + k_{HO^\bullet,H_2O_2} C_{H_2O_2}} \qquad (10)$$

Taking into account that:

$$k_{HO^\bullet,Py} C_{Py} + k_{HO^\bullet,Ac} C_{Ac} \gg k_{HO^\bullet,O_3} C_{O_3} + k_{HO^\bullet,H_2O_2} C_{H_2O_2} \qquad (11)$$

$$k_{HO^\bullet,Py} \approx k_{HO^\bullet,Ac}$$

and

$$k_{HO^\bullet,Py} C_{Py} + k_{HO^\bullet,Py}(C_{Py_o} - C_{Py}) = k_{HO^\bullet,Py} C_{Py_o} \qquad (12)$$

finally,

$$C_{HO^\bullet} = \gamma C_{O_3}^* \qquad (13)$$

So the pyruvic abatement by this system is the contribution of direct photolysis, direct ozonation and oxidation by hydroxyl
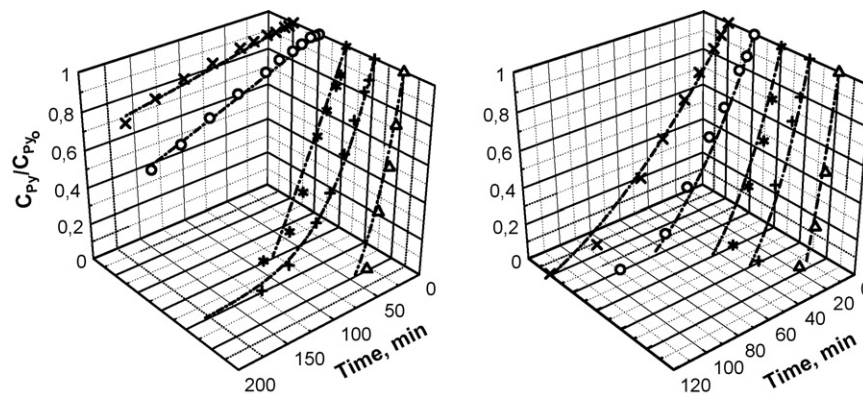

Fig. 8. Oxidation of pyruvic acid. Process modelling (dash–dot curves). (A) Experimental conditions and symbols (data points) as in Fig. 1. (B) The system O_3/UV radiation/perovskite. Experimental conditions (unless indicated): pH 7, $Q_{O_3+O_2} = 40\,\mathrm{L\,h^{-1}}$, $C_{O_3g(inlet)} = 50\,\mathrm{g\,m^{-3}}$, $C_{Perovskite} = 1.0\,\mathrm{g\,L^{-1}}$, $C_{Py_o} = 5 \times 10^{-3}\,\mathrm{mol\,L^{-1}}$; $T = 293\,\mathrm{K}$, $I_o = 4.5 \times 10^{-6}$ Einstein L^{-1} s^{-1} and $L = 4.5\,\mathrm{cm}$. Symbols (data points): ($\times$) $C_{O_3g(inlet)} = 15\,\mathrm{g\,m^{-3}}$; ($\bigcirc$) $C_{O_3g(inlet)} = 30\,\mathrm{g\,m^{-3}}$; ($*$) $C_{O_3g(inlet)} = 50\,\mathrm{g\,m^{-3}}$; (+) $C_{O_3g(inlet)} = 75\,\mathrm{g\,m^{-3}}$; ($\triangle$) $C_{Py_o} = 1 \times 10^{-3}\,\mathrm{mol\,L^{-1}}$.

radicals. The latter pathway represented by:

$$-\frac{dC_{Py}}{dt} = k_{HO^\bullet,Py}\gamma C^*_{O_3}C_{Py} = k_{UV/O_3}C^*_{O_3}C_{Py} \qquad (14)$$

The value of k_{UV/O_3} obtained from the experimental data was $125\,M^{-1}\,min^{-1}$.

Fig. 8A illustrates the simulation of individual systems by considering the expressions 1–14. Additionally, Fig. 8B shows some examples for the system O_3/UV radiation/perovskite obtained by changing the initial concentration of pyruvic acid or the inlet ozone concentration. The complexity of reaction pH was not taken into account and the model was only used for runs conducted at pH 7. The simplistic approach, used to modelling the experimental results, leads to infer two conclusions. On one hand, there is not a synergistic effect when combining ozone, radiation and perovskites, i.e. the final effect is the addition of the systems $UV + UV/O_3 + O_3 + O_3$/perovskites. On the other hand, the pseudo empirical model used acceptably simulates the performance of the system O_3/UV radiation/perovskite under different operating conditions by just considering the ozone equilibrium concentration, $C^*_{O_3}$. The latter amount is a function of inlet ozone concentration according to:

$$C^*_{O_3} = \frac{0.75 C_{O_3 inlet} RT}{H} \qquad (15)$$

where R is the universal gas constant, T is temperature and H is Henry's constant.

4. Conclusions

From the present work the following conclusions can be enumerated:

- From the different oxidation systems described by the combination of ozone, UV radiation and a solid catalyst (perovskites), the photocatalytic ozonation gives the best results in terms of pyruvic acid removal and mineralization degree achieved.
- The photolysis of added hydrogen peroxide also shows an outstanding capacity for pyruvic acid removal, however, mineralization degree highly depends on the initial hydrogen peroxide concentration added at the beginning. From the results obtained, it can be stated that for equal initial concentrations of pyruvic acid and H_2O_2, the mineralization degree obtained is roughly 50%.
- The combination O_3/UV radiation/perovskite is the result of the simple contributions of the systems: $O_3 + UV$ radiation $+ O_3$/perovskite $+ O_3$/UV radiation. The presence of the photo-ozonation stage involves that catalyst concentration shows two opposite effects, for instance a high amount of perovskites increases the catalytic ozonation but decreases the efficiency of the UV radiation.
- A simplistic mathematical model accounting for individual stages is capable of acceptably simulating the system O_3/UV radiation/perovskite under different operating conditions.

Acknowledgements

References

[1] K. Ikehata, M.G. El-Din, Aqueous pesticide degradation by ozonation and ozone-based advanced oxidation processes: a review (part I), Ozone Sci. Eng. 27 (2005) 83–114.

[2] P.R. Gogate, A.B. Pandit, A review of imperative technologies for wastewater treatment. II. Hybrid methods, Adv. Environ. Res. 8 (2004) 553–597.

[3] F.J. Beltrán, Ozone Reaction kinetics for Water and Wastewater Systems, Lewis Publishers/CRC Press Company, Boca Raton, FL, 2004.

[4] R. Andreozzi, V. Caprio, R. Marotta, V. Tufano, Kinetic modeling of pyruvic acid ozonation in aqueous solutions catalyzed by Mn(II) and Mn(IV) ions, Water Res. 35 (2001) 109–120.

[5] H. Bader, J. Hoigne, Determination of ozone in water by the indigo method, Water Res. 15 (1981) 449–456.

[6] F.J. Rivas, M. Carbajo, F.J. Beltrán, B. Acedo, O. Gimeno, Perovskite catalytic ozonation of pyruvic acid in water. Operating conditions influence and kinetics, Appl. Catal. B 62 (2006) 93–103.

[7] F.J. Beltran, B. Acedo, F.J. Rivas, O. Gimeno, Pyruvic acid removal from water by the simultaneous action of ozone and activated carbon, Ozone Sci. Eng. 27 (2005) 159–169.

[8] M. Carbajo, F.J. Beltran, F. Medina, O. Gimeno, F.J. Rivas, Catalytic ozonation of phenolic compounds. The case of gallic acid, Appl. Catal. B 67 (2006) 177–186.

[9] O. Gimeno, M. Carbajo, F.J. Beltran, F.J. Rivas, Phenol and substituted phenols AOPs remediation, J. Hazard. Mater. B119 (2005) 99–108.